ELSEVIER

Applied Numerical Mathematics 33 (2000) 175–181

APPLIED NUMERICAL MATHEMATICS

www.elsevier.nl/locate/apnum

An accurate and efficient spectral method for studies of the dynamical properties of forced, circular shear layers

J.P. Lynov [a,*], K. Bergeron [b], E.A. Coutsias [c], A.H. Nielsen [a]

[a] *Optics and Fluid Dynamics Department, Risø National Laboratory, DK-4000 Roskilde, Denmark*
[b] *Department of Mathematical Sciences, USAF Academy, Colorado Springs, CO 80840, USA*
[c] *Department of Mathematics and Statistics, University of New Mexico, Albuquerque, NM 87131, USA*

Abstract

We present an efficient spectral method for studies of fundamental vortex dynamics in forced, circular shear flows. The numerical results are compared with results from experiments carried out in rotating flows with both planar and parabolic geometries. Due to the high accuracy of the code, it can be determined whether a two-dimensional model is sufficient to describe the experimental results.

Keywords: Numerical simulation; Spectral methods; Asymptotic analysis; Rotating fluids; Vortex dynamics

0. Introduction

In the study of the dynamics of coherent structures, forced circular shear flows offer many desirable features. The inherent quantization of circular geometries due to the periodic boundary conditions makes it possible to design experiments in which the spatial and temporal complexity of the coherent structures can be accurately controlled. A large number of experiments on circular shear layers have been performed in a variety of physical systems, including rotating gases and fluids, and magnetized plasmas (see, e.g., [1,2] for a list of references). A number of theoretical and numerical investigations of these systems have also been performed. However, the quantitative agreement between the results from these theoretical and numerical studies and the experimental results have been rather poor. Up till now, it has not been possible to determine whether the discrepancies were caused by inadequate physical modeling or by insufficient numerical schemes based on low order methods with low resolution. In this paper, an accurate and efficient spectral method is presented which reduces the errors in the numerical solutions so much that conclusions can be drawn directly concerning the validity of the model equations.

* Corresponding author. E-mail: jens-peter.lynov@risoe.dk

0168-9274/00/$20.00
PII: S0168-9274(99)00081-1

1. Experimental test cases and model equations

We will validate our numerical scheme against two different fluid experiments. In both experimental setups, a radially localized shear forcing of the flow is produced by a differential rotation of an inner and an outer part of the mechanical structure containing the flow. The first test case [3,7] has a planar geometry, while the second [8] is carried out in a parabolic shaped tank. The main control parameter characterizing these flows is the Reynolds number,

$$Re = \frac{\Delta\Omega a e}{\nu}. \tag{1}$$

Here, $\Delta\Omega$ is the difference in angular velocity between the inner and outer flow, a is the radius at which the forcing is introduced, e is the width of the shear layer, and ν the kinematic viscosity. The shear layer aspect ratio, $\Gamma = a/e$, also plays a role in determining the transitions, since Γ is a measure of how important shear curvature is, with smaller values corresponding to flows where curvature effects are more pronounced.

As described in the papers on the experiments, the flows in the two cases can be modeled by the same two-dimensional set of equations. These consist of the Charney equation in the infinite Rossby radius limit

$$\frac{\partial\omega}{\partial t} + J(\omega,\psi) - \frac{\beta}{r}\frac{\partial\psi}{\partial\theta} = \nu\nabla^2\omega + c(\omega^* - \omega), \tag{2}$$

and the Poisson equation

$$\nabla^2\psi = -\omega. \tag{3}$$

In these equations, we have introduced the scalar vorticity ω, the stream function ψ, and the Jacobian

$$J(f,g) \equiv \frac{1}{r}\left(\frac{\partial f}{\partial r}\frac{\partial g}{\partial\theta} - \frac{\partial g}{\partial r}\frac{\partial f}{\partial\theta}\right).$$

The constant β in (2) measures the effect of the varying Coriolis force in the parabolic tank [8] and is zero in the planar case [3,7]. The external forcing function, ω^*, in (2) is an axisymmetric function that enters the Eckman forcing term, and the constant c in front of this term is different in the two test cases.

In both experiments the flow is confined radially between two vertical walls at some distance from the radius of forcing. In order to investigate the effect of boundary layers at these walls, we have solved (2), (3) subject to both free-slip and no-slip boundary conditions.

2. Numerical scheme

In the numerical solution of (2), (3) a spectral method is employed in which all functions are expanded in the form

$$g(r,\theta,t) = \sum_{m=0}^{M}\sum_{n=-N/2}^{N/2-1} g_{mn}(t)T_m(r)\mathrm{e}^{\mathrm{i}n\theta}, \tag{4}$$

where M and N are the orders of truncation and $T_m(r)$ (with normalized r) is the mth degree Chebyshev polynomial.

For the time integration of (2) we have used a 3rd order "Stiffly Stable" scheme [6], which is a mixed explicit/implicit time integration method. Thus, for each time step two elliptic equations, the Poisson equation (3) and the Helmholtz equation originating from the implicit term, must be solved. These equations are solved by an invertible integral operator method [4] which very efficiently solves the equations in $O(MN)$ operations with high accuracy even at high truncations ($M \sim N \sim 1024$). The invertible integral operator method is developed for ordinary differential equations with varying, rational function coefficients. It decomposes the solution into a "particular solution" and a null-space correction taking care of the boundary conditions. In this way, the method is well suited for domain decomposition since it only needs to exchange boundary information between neighboring domains.

As mentioned above, both free-slip and no-slip boundary conditions have been implemented in our scheme. The no-slip conditions are not easily introduced since (2) and (3) describe the flow in the vorticity-stream function formulation, while the no-slip condition expresses a constraint on the flow velocity. Actually, transcribing the no-slip velocity condition to the stream function causes the Poisson equation (3) to be overdetermined. We have previously developed an accurate integral solvability constraint method [5] to resolve this apparent overdeterminancy. In this method, the coefficients belong to the solvability constraints are independent of viscosity and mode number truncation, and they are calculated in a pre-processing stage. This way, imposing the solvability constraints during the dynamical calculations add virtually no computational overhead.

In the explicit calculation of the nonlinear convection term, the products are calculated in point space and the result fully de-aliased using the standard $2/3$ truncation scheme. The accuracy of the full numerical simulations is diagnosed by comparing the instantaneous temporal derivatives of the global quantities: energy, enstrophy and angular momentum, obtained by time-stepping the simulation with the analytical expressions for these quantities, and very high accuracies are obtained.

3. Asymptotic analysis

In addition to complete numerical simulations of the flows following (2) and (3) we have also performed a weakly nonlinear analysis of the planar flows (with $\beta = 0$ in (2)) near the critical Reynolds number, Re_c, where the flow undergoes the first bifurcation. In this analysis, we are guided by the results from the experiments [3,7] and from the full simulations which demonstrate that the flow is stable to radially symmetric perturbations at any Reynolds number, but becomes unstable to azimuthal perturbations therefore, introduce the small parameter ε such that $\nu = 1/(Re_c + \varepsilon^2) = \nu_c(1 - \varepsilon^2\nu_c + O(\varepsilon^4))$.

We also introduce the slow time scale $\tau = \varepsilon t$ and expand the flow fields in the form

$$g(r,\theta,t) = g_0(r) + \sum_{k=1}^{3} \varepsilon^k g_k(r,\theta,t,\tau) + O(\varepsilon^4); \tag{5}$$

here g stands for either ω or ψ. The slow time scale is suggested as usual by the dependence of the unstable eigenvalues on Re in the vicinity of $Re = Re_c$.

The analysis of the $O(\varepsilon^0)$ and $O(\varepsilon^1)$ problems gives the basic linearized stability picture. This determines the value of Re_c, the linear eigenfunctions and the linear growth rates. To $O(\varepsilon^2)$ the perturbation equations produce nonresonant second (and zero) harmonic corrections, but to $O(\varepsilon^3)$ the

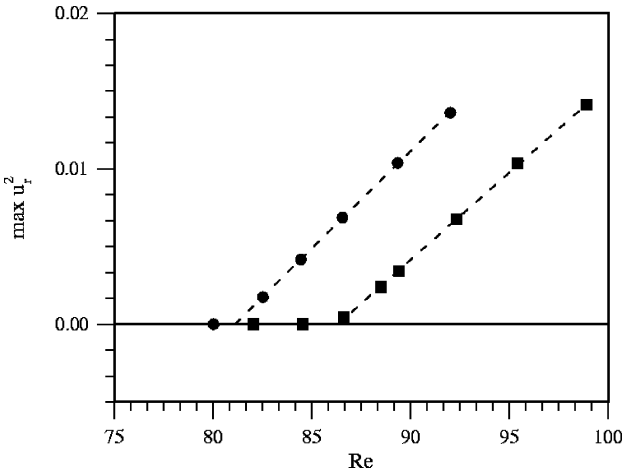

Fig. 1. Supercritical bifurcation near the critical Reynolds number for $a = 3$, $\Gamma = 6.5$. The black circles mark the values of the saturated amplitude of the square of the maximal radial velocity, $\max u_r^2$, for different values of the Reynolds number *Re* and free-slip boundary conditions. The black squares show similar results for no-slip boundary conditions. The dashed lines indicate linear, least square fits to the points with non-axisymmetric flows.

interaction of these harmonics with the fundamental produces resonant (secular) terms. Suppressing these terms leads to

$$\frac{\mathrm{d}A}{\mathrm{d}\tau} = \alpha A + \xi |A|^2 A, \tag{6}$$

which is the Landau equation for the saturation behavior of the complex amplitude, $A(\tau)$, of the neutral mode. Further details on the asymptotic analysis can be found in [2].

4. Numerical results

Fig. 1 shows the numerical results for the nonlinear saturation of the perturbation near the first bifurcation from the axisymmetric state. The calculations were initialized by exciting the first 20 azimuthal modes with random phases and low amplitudes. For *Re* less than a well-defined critical value, Re_c, all the azimuthal modes die out and an axisymmetric state is restored. For *Re* values not too far above Re_c, an $n = 5$ mode is excited in agreement with the linear analysis for $\Gamma = 6.5$ and $a = 3$. After a transient period, during which the stable modes die out, the $n = 5$ perturbation grows to a finite amplitude and saturates. It is clearly seen that the saturated amplitudes of u_r grow as $(Re - Re_c)^{(1/2)}$ characteristic for the supercritical bifurcation assumed in the asymptotic analysis in Section 3.

The intersections of the dashed lines in Fig. 1 with the *Re*-axis give good estimates of Re_c. The values for Re_c found this way are 81.1 ± 0.1 (free-slip) and $Re_c = 86.3 \pm 0.1$ (no-slip). These values are in good agreement with the results from the asymptotic analysis, which gives $Re_c = 80.6$ and $Re_c = 86.18$ for the free-slip and no-slip cases, respectively. Experimentally, [7] found $Re_c = 85 \pm 5$, while [3] reported $Re_c = 80 \pm 2$. We note that in the numerical simulations of [3], the critical Reynolds number was found to be $Re_c \approx 60$ for $\Gamma = 6.5$ which is far from the experimental value. Given the results presented in

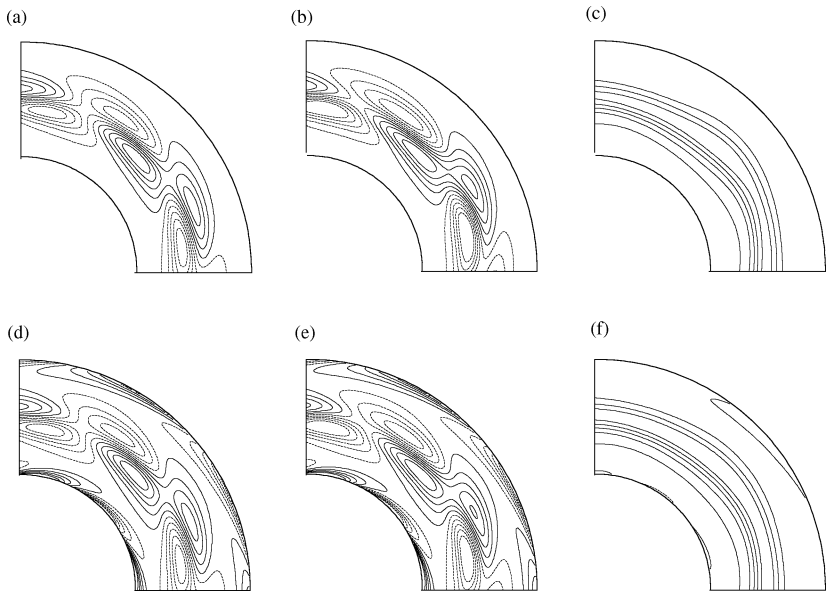

Fig. 2. Vorticity fields of a section of the first unstable mode for $a = 3$, $\Gamma = 6.5$. Dashed lines indicate negative values and full lines positive values. (a)–(c) Free-slip boundary conditions; (d)–(f) no-slip conditions. (a), (d) Eigenfunctions for the marginally stable case from linear analysis; (b), (e) saturated perturbation from full numerical simulation at $Re = 89.32$; (c), (f) total saturated field from the same numerical simulation as in (b), (e). In all the figures, the amplitude has been normalized to 1.

this paper, it is clear that this large discrepancy is not due physical effects missing from the model equations (2), (3) but must be ascribed to the crude numerical scheme used in [3].

In Fig. 2, vorticity fields corresponding to the eigenfunctions from linear analysis are shown for both free-slip and no-slip boundary conditions. Also shown are the saturated perturbation and the total saturated field from the full simulations. The good agreement between the linear results and the results from the full numerical simulations is obvious. We have also calculated the saturated perturbation for the other *Re* values represented in Fig. 1 and found that the geometry of the fields corresponding to the two different boundary conditions only changed slightly for $Re_c < Re < 100$. The temporal growth and saturation of the amplitude of the perturbation for slightly unstable flows was compared with the Landau equation (6) derived in Section 3 and an excellent agreement was found.

When *Re* is increased further above Re_c than in the simulations shown in Fig. 1, a series of symmetry breaking bifurcations occur. An example of such a bifurcation is shown in Fig. 3. We have found that during all bifurcations, including the first bifurcation from the axisymmetric state, there are clear drops in the energy and the enstrophy of the flow. During spin-down the flow exhibits a clear hysteresis in agreement with the experimental observations. In the simulations, the inverse bifurcations only occur when additional noise is added to the flow.

For the second test case in the parabolic geometry the generic flow behavior is very similar to the behavior in the first test case. In Fig. 4 we show a full sequence of bifurcations. Again in this case we see the fine agreement between the numerical simulations and the experiment.

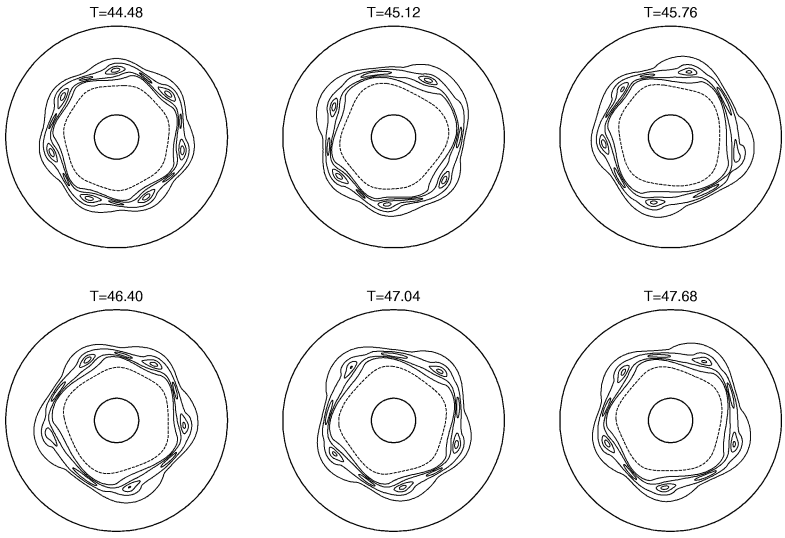

Fig. 3. Symmetry breaking transition during spin-up.

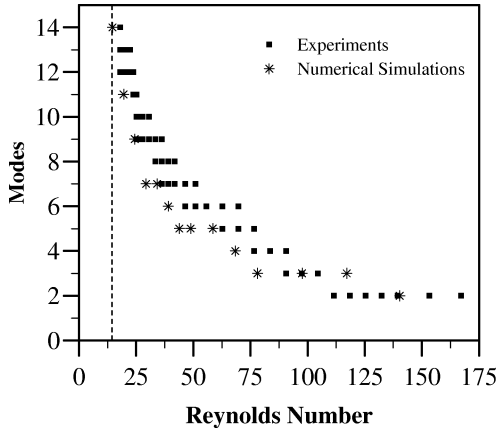

Fig. 4. Sequence of bifurcations in a parabolic tank.

5. Conclusion

We have presented an accurate and efficient spectral method for studies of the dynamical properties of forced, circular shear layers. The code has been tested against theoretical results from asymptotic analysis and verified against two different experimental test cases. Due the high agreement achieved in all cases, we are able to conclude that the two-dimensional model equations (2), (3) are fully capable of describing the complex vortex dynamics in the shear flows, at least in the cases where we have able to make comparisons.

Acknowledgements

The authors are grateful to J.S. Hesthaven for many valuable discussions on the accuracy of differentiation operations in Chebyshev spectral methods. This work was supported in part by DOE Grant DE-FG03-92ER25128 and by the Danish Science Research Councils.

References

[1] K. Bergeron, E.A. Coutsias, J.P. Lynov, A.H. Nielsen, Self organization in circular shear layers, Phys. Scripta T67 (1996) 33–37.
[2] K. Bergeron, E.A. Coutsias, J.P. Lynov, A.H. Nielsen, Dynamical properties of forced shear layers in an annular geometry, J. Fluid Mech. 402 (2000) 255–289.
[3] J.M. Chomas, M. Rabaud, C. Basdevant, Y. Couder, Experimental and numerical investigation of a forced circular shear layer, J. Fluid Mech. 187 (1988) 115–140.
[4] E.A. Coutsias, T. Hagstrom, D. Torres, An efficient spectral method for ordinary differential equations with rational function coefficients, Math. Comp. 65 (1995) 611–635.
[5] E.A. Coutsias, J.P. Lynov, Fundamental interactions of vortical structures with boundary layers in two-dimensional flows, Phys. D 51 (1991) 482–497.
[6] G.E. Karniadakis, M. Israeli, S.A. Orszag, High-order splitting methods for the incompressible Navier–Stokes equations, J. Comput. Phys. 97 (1991) 414–443.
[7] M. Rabaud, Y. Couder, A shear-flow instability in a circular geometry, J. Fluid Mech. 136 (1983) 59–82.
[8] J.A. van de Konijnenberg, A.H. Nielsen, J. Juul Rasmussen, B. Stenum, Shear-flow instability in a rotating fluid, J. Fluid Mech. 387 (1999) 177–204.